


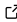
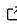
SatRbedo: An R package for retrieving snow and ice albedo from optical satellite imagery

Pablo Fuchs¹[¶], Ruzica Dadic^{2,3}, Shelley MacDonell¹, Heather Purdie¹, Brian Anderson³, and Marwan Katurji¹

¹ School of Earth & Environment, University of Canterbury, Christchurch, New Zealand ² WSL Institute for Snow and Avalanche Research, Davos Dorf, Switzerland ³ Antarctic Research Centre, Victoria University, Wellington, New Zealand [¶] Corresponding author

DOI: [10.xxxxxx/draft](https://doi.org/10.xxxxxx/draft)

Software

- [Review](#) 
- [Repository](#) 
- [Archive](#) 

Editor: [Ethan White](#)  

Reviewers:

- [@dlebauer](#)
- [@DS4Ag](#)

Submitted: 12 June 2025

Published: unpublished

License

Authors of papers retain copyright and release the work under a Creative Commons Attribution 4.0 International License ([CC BY 4.0](#)).

Summary

Albedo is a key variable determining the amount of solar radiation absorbed by snow and ice surfaces. As such, it influences meltwater production, glacier mass balance, and the energy exchange between the Earth and the atmosphere (Hock, 2005; Jonsell et al., 2003). Satellite remote sensing has been widely recognized as the best practical approach for monitoring and mapping surface albedo across different spatial and temporal scales (Lin et al., 2022; Urraca et al., 2023). Here, we present the SatRbedo R package: an extensible, standalone toolbox for retrieving snow and ice albedo from optical satellite imagery. The package includes tools for image preprocessing, converting nadir satellite observations to off-nadir values using view-angle corrections, detecting topographic shadows, discriminating snow and ice surfaces, correcting for topographic effects and the anisotropic behavior of reflected radiation of glacier snow and ice, and converting narrowband to broadband albedo. The toolbox has a modular structure that allows for changing the implemented routines and provides output that can be used independently or as input to other functions. SatRbedo is designed to work with medium-resolution satellite data (e.g., Landsat and Sentinel-2), although data from different satellite sensors can also be used.

Statement of need

The land surface albedo is an essential climate variable that controls the partitioning of radiative energy between the surface and the atmosphere (Bojinski et al., 2014; Radeloff et al., 2024). Albedo is the hemispherically integrated reflectance representing the proportion of the incoming solar radiation reflected from a unit surface area (Budyko, 1969; Schaepman-Strub et al., 2006). In the cryosphere, albedo ranges from <0.1 for debris-covered ice to 0.3-0.4 for bare ice to ~0.5 for aged, wet snow to >0.9 for fresh, dry snow (Cuffey & Paterson, 2010).

Snow and ice albedo depend on the inherent optical properties of the surface (including snow grain size and shape, snowpack thickness, surface roughness, and water and impurity content) and are also influenced by environmental conditions (apparent albedo), including the angular and spectral distribution of solar radiation, topography, the underlying substrate for thin snow cover, and cloud cover (Warren, 2019; Whicker et al., 2022).

Broadband albedo can be measured in the field using observations from a pyranometer pair, one looking upward and the other looking downward (Driemel et al., 2018; Picard et al., 2020). Alternatively, albedo can be estimated using a combination of snow/ice properties and radiative transfer models (Flanner et al., 2021; Whicker et al., 2022) and from satellite remote sensing (Bertoncini et al., 2022; Fugazza et al., 2016).

Instrumentation deployed on towers and automatic weather stations can provide high-quality albedo data with high-temporal resolution at a single location. However, the pyranometer footprint limits the spatial extrapolation of the albedo data (Berg et al., 2020).

Coupled snow radiative transfer and snowpack models can simulate the temporal and spatial evolution of snow optical properties. However, these coupled models are associated with high computational costs and limited spatial resolution (Gaillard et al., 2025). Also, these models require input data that is often spatially variable and unavailable most of the time.

Remote sensing offers the best option for studying the changes in albedo, accounting for the high variability in space and time (Berg et al., 2020). Satellite albedo retrievals typically comprise three steps: (1) atmospheric correction, (2) modeling of the angular reflectance, and (3) narrow-to-broadband albedo conversion (Carlsen et al., 2020; Qu et al., 2015). The algorithms for atmospheric correction (Doxani et al., 2023; Vermote et al., 2016), modeling of the angular reflectance distribution (Lucht et al., 2000; Ren et al., 2021), and narrow-to-broadband albedo conversion (Knap et al., 1999; Li et al., 2018; Liang, 2001) are well-established and validated in a number of case studies. In addition to these steps, satellite image pre-processing and topographic correction are necessary for homogenizing the input data and minimizing the effects of slope and aspect on albedo, respectively.

Several workflows have been proposed to address these processing steps (e.g., Klok et al., 2003; Shuai et al., 2011). However, research code supporting their implementation is not always readily available. This paper introduces the SatRbedo package, which implements a workflow in R to estimate snow and ice albedo from satellite data.

Implementation

SatRbedo consists of tools that run in a processing pipeline (Figure 1).

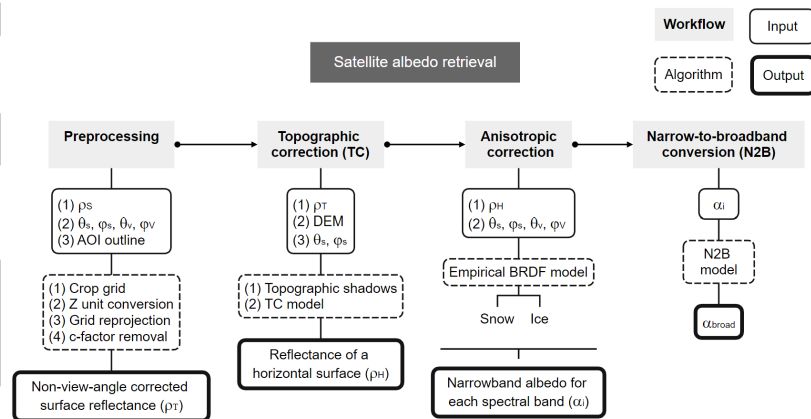


Figure 1: Flowchart of the satellite albedo retrieval workflow. It includes four processing steps: (1) pre-processing, (2) topographic correction, (3) anisotropic correction, and (4) narrow-to-broadband albedo conversion. The details of the methods are described in the text.

First, it takes application-ready surface reflectance data (ρ_s) derived from top-of-atmosphere reflectance, satellite (φ_v, θ_v) and solar (φ_s, θ_s) azimuth and zenith angles, and an outline of the area of interest (AOI) to perform the following pre-processing steps: (1) crop the satellite grids to a specified extent; (2) convert data from integer to floating point; (3) re-project grids to a common coordinate system; and (4) convert nadir satellite observations to off-nadir values using view-angle corrections based on the c-factor method (Roy et al., 2016).

Subsequently, the non-view-angle corrected surface reflectance (ρ_T) is corrected for the effects

of topography to obtain the equivalent reflectance values over flat terrain (ρ_H). Two empirical methods are provided in SatRbedo: (1) the rotation model proposed by Tan et al. (2013) and the C-correction model (Teillet et al., 1982). These algorithms are suitable for mountain environments with rugged topography and non-Lambertian surface properties and require a digital elevation model (DEM) and the solar azimuth and zenith angles as input data. The two models assume a linear relationship between reflectance and the solar incidence angle on an inclined surface. Additionally, a tool is provided to remove topographic shadows (self and cast shadows) using the vectorial algebra algorithms proposed by Corripio (2003).

The next step accounts for the anisotropic reflection of snow and ice. For a given surface type, the correction is carried out using an empirical model of the Bidirectional Reflectance Distribution Function (BRDF) that depends on the wavelength bands and the view-solar geometry. SatRbedo provides two different models: (1) the BRDF models of Koks (2001) for snow and Greuell & De Ruyter De Wildt (1999) for ice when the green and near-infrared (NIR) bands are used, and (2) the parameterizations proposed by Ren et al. (2021) for the combination of the blue, red, NIR, and shortwave-infrared bands. To distinguish between snow and ice surfaces, we need to calculate the Normalized Difference Snow Ice Index (NDSII, Keshri et al., 2009). The subsequent discrimination between snow and ice is performed using an automatic threshold selection method based on the Otsu algorithm (Otsu, 1979).

Finally, broadband albedo can be calculated from narrowband albedo using three empirical relationships: Knap et al. (1999), Liang (2001), and Feng et al. (2023).

Future development

It is expected that active development on SatRbedo will continue in the future through the incorporation of the newest tools and methods as they become available, as well as through the active participation of the research community through the software repository platform. Developments in progress include a kernel-based semiempirical BRDF model and new snow and snow-free narrow-to-broadband albedo conversion algorithms.

Acknowledgements

This research was supported by a University of Canterbury Doctoral Scholarship. The authors wish to acknowledge using the terra package that provided the raster data handling infrastructure on which SatRbedo was built. We also thank Javier Corripio, who wrote the original vectorial algebra algorithms for computing topographic shading on complex terrain.

References

- Berg, L. K., Long, C. N., Kassianov, E. I., Chand, D., Tai, S., Yang, Z., Riihimäki, L. D., Biraud, S. C., Tagestad, J., Matthews, A., Mendoza, A., Mei, F., Tomlinson, J., & Fast, J. D. (2020). Fine-Scale Variability of Observed and Simulated Surface Albedo Over the Southern Great Plains. *Journal of Geophysical Research: Atmospheres*, 125(7), e2019JD030559. <https://doi.org/10.1029/2019JD030559>
- Bertoncini, A., Aubry-Wake, C., & Pomeroy, J. W. (2022). Large-area high spatial resolution albedo retrievals from remote sensing for use in assessing the impact of wildfire soot deposition on high mountain snow and ice melt. *Remote Sensing of Environment*, 278, 113101. <https://doi.org/10.1016/j.rse.2022.113101>
- Bojinski, S., Verstraete, M., Peterson, T. C., Richter, C., Simmons, A., & Zemp, M. (2014). The concept of essential climate variables in support of climate research, applications, and policy. *Bulletin of the American Meteorological Society*, 95(9), 1431–1443. <https://doi.org/10.1175/BAMS-D-13-00047.1>

- 116 Budyko, M. I. (1969). The effect of solar radiation variations on the climate of the Earth.
117 *Tellus*, 21(5), 611–619. <https://doi.org/10.1111/j.2153-3490.1969.tb00466.x>
- 118 Carlsen, T., Birnbaum, G., Ehrlich, A., Helm, V., Jäkel, E., Schäfer, M., & Wendisch, M.
119 (2020). Parameterizing anisotropic reflectance of snow surfaces from airborne digital
120 camera observations in Antarctica. *The Cryosphere*, 14(11), 3959–3978. <https://doi.org/10.5194/tc-14-3959-2020>
121
- 122 Corripio, J. G. (2003). Vectorial algebra algorithms for calculating terrain parameters from
123 DEMs and solar radiation modelling in mountainous terrain. *International Journal of*
124 *Geographical Information Science*, 17(1), 1–23. <https://doi.org/10.1080/713811744>
- 125 Cuffey, K., & Paterson, W. S. B. (2010). *The physics of glaciers* (4th ed). Butterworth-
126 Heinemann/Elsevier. ISBN: 978-0-12-369461-4
- 127 Doxani, G., Vermote, E. F., Roger, J.-C., Skakun, S., Gascon, F., Collison, A., De Keukelaere,
128 L., Desjardins, C., Frantz, D., Hagolle, O., Kim, M., Louis, J., Pacifici, F., Pflug, B.,
129 Poilvé, H., Ramon, D., Richter, R., & Yin, F. (2023). Atmospheric Correction Inter-
130 comparison eXercise, ACIX-II Land: An assessment of atmospheric correction processors
131 for Landsat 8 and Sentinel-2 over land. *Remote Sensing of Environment*, 285, 113412.
132 <https://doi.org/10.1016/j.rse.2022.113412>
- 133 Driemel, A., Augustine, J., Behrens, K., Colle, S., Cox, C., Cuevas-Agulló, E., Denn, F.
134 M., Duprat, T., Fukuda, M., Grobe, H., Haefelin, M., Hodges, G., Hyett, N., Ijima,
135 O., Kallis, A., Knap, W., Kustov, V., Long, C. N., Longenecker, D., ... König-Langlo,
136 G. (2018). Baseline Surface Radiation Network (BSRN): Structure and data description
137 (1992–2017). *Earth System Science Data*, 10(3), 1491–1501. <https://doi.org/10.5194/essd-10-1491-2018>
138
- 139 Feng, S., Cook, J. M., Onuma, Y., Naegeli, K., Tan, W., Anesio, A. M., Benning, L.
140 G., & Tranter, M. (2023). Remote sensing of ice albedo using harmonized Landsat
141 and Sentinel 2 datasets: validation. *International Journal of Remote Sensing*, 1–29.
142 <https://doi.org/10.1080/01431161.2023.2291000>
- 143 Flanner, M. G., Arnheim, J. B., Cook, J. M., Dang, C., He, C., Huang, X., Singh, D., Skiles,
144 S. M., Whicker, C. A., & Zender, C. S. (2021). SNICAR-ADv3: A community tool for
145 modeling spectral snow albedo. *Geoscientific Model Development*, 14(12), 7673–7704.
146 <https://doi.org/10.5194/gmd-14-7673-2021>
- 147 Fugazza, D., Senese, A., Azzoni, R. S., Maugeri, M., & Diolaiuti, G. A. (2016). Spatial
148 distribution of surface albedo at the Forni Glacier (Stelvio National Park, Central Italian
149 Alps). *Cold Regions Science and Technology*, 125, 128–137. <https://doi.org/10.1016/j.coldregions.2016.02.006>
150
- 151 Gaillard, M., Vionnet, V., Lafaysse, M., Dumont, M., & Ginoux, P. (2025). Improving large-
152 scale snow albedo modeling using a climatology of light-absorbing particle deposition. *The*
153 *Cryosphere*, 19(2), 769–792. <https://doi.org/10.5194/tc-19-769-2025>
- 154 Greuell, W., & De Ruyter De Wildt, M. (1999). Anisotropic reflection by melting glacier ice:
155 Measurements and parametrizations in Landsat TM Bands 2 and 4. *Remote Sensing of*
156 *Environment*, 70(3), 265–277. [https://doi.org/10.1016/S0034-4257\(99\)00043-7](https://doi.org/10.1016/S0034-4257(99)00043-7)
- 157 Hock, R. (2005). Glacier melt: A review of processes and their modelling. *Progress in*
158 *Physical Geography: Earth and Environment*, 29(3), 362–391. <https://doi.org/10.1191/0309133305pp453ra>
159
- 160 Jonsell, U., Hock, R., & Holmgren, B. (2003). Spatial and temporal variations in albedo on
161 Storglaciären, Sweden. *Journal of Glaciology*, 49(164), 59–68. <https://doi.org/10.3189/172756503781830980>
162
- 163 Keshri, A. K., Shukla, A., & Gupta, R. P. (2009). ASTER ratio indices for supraglacial terrain

- mapping. *International Journal of Remote Sensing*, 30(2), 519–524. <https://doi.org/10.1080/01431160802385459>
- Klok, E. J. (Lisette)., Greuell, W., & Oerlemans, J. (2003). Temporal and spatial variation of the surface albedo of Morteratschgletscher, Switzerland, as derived from 12 Landsat images. *Journal of Glaciology*, 49(167), 491–502. <https://doi.org/10.3189/172756503781830395>
- Knap, W. H., Reijmer, C. H., & Oerlemans, J. (1999). Narrowband to broadband conversion of Landsat TM glacier albedos. *International Journal of Remote Sensing*, 20(10), 2091–2110. <https://doi.org/10.1080/014311699212362>
- Koks, M. (2001). *Anisotropic reflection of radiation by melting snow. Landsat TM bands 2 and 4* [Master's thesis]. Universiteit Utrecht. Instituut voor Marien en Atmosferisch Onderzoek Utrecht (IMAU).
- Li, Z., Erb, A., Sun, Q., Liu, Y., Shuai, Y., Wang, Z., Boucher, P., & Schaaf, C. (2018). Preliminary assessment of 20-m surface albedo retrievals from Sentinel-2A surface reflectance and MODIS/VIRS surface anisotropy measures. *Remote Sensing of Environment*, 217, 352–365. <https://doi.org/10.1016/j.rse.2018.08.025>
- Liang, S. (2001). Narrowband to broadband conversions of land surface albedo I: Algorithms. *Remote Sensing of Environment*, 76(2), 213–238. [https://doi.org/10.1016/S0034-4257\(00\)00205-4](https://doi.org/10.1016/S0034-4257(00)00205-4)
- Lin, X., Wu, S., Chen, B., Lin, Z., Yan, Z., Chen, X., Yin, G., You, D., Wen, J., Liu, Q., Xiao, Q., Liu, Q., & Laforezza, R. (2022). Estimating 10-m land surface albedo from Sentinel-2 satellite observations using a direct estimation approach with Google Earth Engine. *ISPRS Journal of Photogrammetry and Remote Sensing*, 194, 1–20. <https://doi.org/10.1016/j.isprsjprs.2022.09.016>
- Lucht, W., Schaaf, C. B., & Strahler, A. H. (2000). An algorithm for the retrieval of albedo from space using semiempirical BRDF models. *IEEE Transactions on Geoscience and Remote Sensing*, 38(2), 977–998. <https://doi.org/10.1109/36.841980>
- Otsu, N. (1979). A Threshold Selection Method from Gray-Level Histograms. *IEEE Transactions on Systems, Man, and Cybernetics*, 9(1), 62–66. <https://doi.org/10.1109/TSMC.1979.4310076>
- Picard, G., Dumont, M., Lamare, M., Tuzet, F., Larue, F., Pirazzini, R., & Arnaud, L. (2020). Spectral albedo measurements over snow-covered slopes: Theory and slope effect corrections. *The Cryosphere*, 14(5), 1497–1517. <https://doi.org/10.5194/tc-14-1497-2020>
- Qu, Y., Liang, S., Liu, Q., He, T., Liu, S., & Li, X. (2015). Mapping surface broadband albedo from satellite observations: A review of literatures on algorithms and products. *Remote Sensing*, 7(1), 990–1020. <https://doi.org/10.3390/rs70100990>
- Radeloff, V. C., Roy, D. P., Wulder, M. A., Anderson, M., Cook, B., Crawford, C. J., Friedl, M., Gao, F., Gorelick, N., Hansen, M., Healey, S., Hostert, P., Hulley, G., Huntington, J. L., Johnson, D. M., Neigh, C., Lyapustin, A., Lymburner, L., Pahlevan, N., ... Zhu, Z. (2024). Need and vision for global medium-resolution Landsat and Sentinel-2 data products. *Remote Sensing of Environment*, 300, 113918. <https://doi.org/10.1016/j.rse.2023.113918>
- Ren, S., Miles, E. S., Jia, L., Menenti, M., Kneib, M., Buri, P., McCarthy, M. J., Shaw, T. E., Yang, W., & Pellicciotti, F. (2021). Anisotropy parameterization development and evaluation for glacier surface albedo retrieval from satellite observations. *Remote Sensing*, 13(9), 1714. <https://doi.org/10.3390/rs13091714>
- Roy, D. P., Zhang, H. K., Ju, J., Gomez-Dans, J. L., Lewis, P. E., Schaaf, C. B., Sun, Q., Li, J., Huang, H., & Kovalskyy, V. (2016). A general method to normalize Landsat reflectance data to nadir BRDF adjusted reflectance. *Remote Sensing of Environment*, 176, 255–271. <https://doi.org/10.1016/j.rse.2016.01.023>

- 212 Schaepman-Strub, G., Schaepman, M. E., Painter, T. H., Dangel, S., & Martonchik, J. V.
213 (2006). Reflectance quantities in optical remote sensing—definitions and case studies.
214 *Remote Sensing of Environment*, 103(1), 27–42. <https://doi.org/10.1016/j.rse.2006.03.002>
- 215 Shuai, Y., Masek, J. G., Gao, F., & Schaaf, C. B. (2011). An algorithm for the retrieval
216 of 30-m snow-free albedo from Landsat surface reflectance and MODIS BRDF. *Remote*
217 *Sensing of Environment*, 115(9), 2204–2216. <https://doi.org/10.1016/j.rse.2011.04.019>
- 218 Tan, B., Masek, J. G., Wolfe, R., Gao, F., Huang, C., Vermote, E. F., Sexton, J. O., & Ederer, G.
219 (2013). Improved forest change detection with terrain illumination corrected Landsat images.
220 *Remote Sensing of Environment*, 136, 469–483. <https://doi.org/10.1016/j.rse.2013.05.013>
- 221 Teillet, P. M., Guindon, B., & Goodenough, D. G. (1982). On the Slope-Aspect Correction
222 of Multispectral Scanner Data. *Canadian Journal of Remote Sensing*, 8(2), 84–106.
223 <https://doi.org/10.1080/07038992.1982.10855028>
- 224 Urraca, R., Lanconelli, C., Cappucci, F., & Gobron, N. (2023). Assessing the Fitness of
225 Satellite Albedo Products for Monitoring Snow Albedo Trends. *IEEE Transactions on*
226 *Geoscience and Remote Sensing*, 61, 1–17. <https://doi.org/10.1109/TGRS.2023.3281188>
- 227 Vermote, E., Justice, C., Claverie, M., & Franch, B. (2016). Preliminary analysis of the
228 performance of the Landsat 8/OLI land surface reflectance product. *Remote Sensing of*
229 *Environment*, 185, 46–56. <https://doi.org/10.1016/j.rse.2016.04.008>
- 230 Warren, S. G. (2019). Optical properties of ice and snow. *Philosophical Transactions of the*
231 *Royal Society A: Mathematical, Physical and Engineering Sciences*, 377(2146), 20180161.
232 <https://doi.org/10.1098/rsta.2018.0161>
- 233 Whicker, C. A., Flanner, M. G., Dang, C., Zender, C. S., Cook, J. M., & Gardner, A. S.
234 (2022). SNICAR-ADv4: A physically based radiative transfer model to represent the
235 spectral albedo of glacier ice. *The Cryosphere*, 16(4), 1197–1220. <https://doi.org/10.5194/tc-16-1197-2022>
236